Indian Journal of Pure & Applied Physics
Vol. 55, September 2017, pp. 638-648

Electronic structure investigations of 1-amino-2,6-dimethylpiperidine by NMR spectral studies by *ab initio* and DFT calculations

D Cecily Mary Glory[a,b], R Madivanane[c] & K Sambathkumar[d]*

[a]R & D centre, Bharathar University, Coimbatore 641 046, India
[b]Idhaya College of Arts and Science for Women, Puducherry 605 008, India
[c]Department of Physics, Mahatma Government College, Maye, Puducherry 673 311, India
[d]Post Graduate & Research Department of Physics, A A Government Arts College, Villupuram 605 602, India

Received 20 September 2016; accepted 14 February 2017

In this work, a combined experimental and theoretical study on molecular structure, vibrational spectra of 1-amino-2,6-dimethylpiperidine (ADP) has been reported. The FTIR and FT-Raman spectrum have been recorded in the region 4000-400 cm^{-1} and 3500-50 cm^{-1}, respectively. The molecular geometry, harmonic vibrational frequencies and bonding features of ADP have been calculated by using *ab initio*/HF and density functional theory/B3LYP methods with 6-31+G(d,p) basis set. A detailed interpretation of the FTIR, FT-Raman, NMR spectra of ADP has also been reported. Natural bond orbital analysis has been carried out to explain the charge transfer or delocalization of charge due to the intra-molecular interactions. Energy of the highest occupied molecular (HOMO) orbital and lowest unoccupied (LUMO) molecular orbital have been predicted.

Keywords: FTIR, FT-Raman, ADP, HOMO-LUMO, NBO, NMR

1 Introduction

Piperidines are an important group of heterocyclic compounds in the field of medicinal chemistry owing to the fact that these can frequently be recognized in the structure of numerous naturally occurring alkaloid and synthetic compounds with interesting biological and pharmacological properties. Piperidine derivatives were also reported to possess analgesic[1,2], anti-inflammatory[2] central nervous system[3-7] local anaesthetic[8], anticancer[9] and antimicrobial activity[10]. Piperidine nucleus is also found in drugs as raloxifene, minaxidil[11] and as a raw material for preparing epoxy resins, corrosion inhibitors and autioxidant[12]. The vibrational studies of piperidine on theoretical studies of density functional calculations were also reported[13-20]. Our literature survey also reveals that no theoretical calculations or detailed vibrational infrared and Raman analysis have been performed on 1-amino-2,6-dimethylpiperidine (ADP) molecule so far. A systematic study on the vibrational spectra and structure will aid in understanding the vibrational modes of this title molecule. So, in this study, the vibrational wave numbers, geometrical parameters, modes of vibrations, NMR and electrostatic potential also provide information about electronic effects of ADP molecule were investigated by using *ab initio*/HF and DFT/B3LYP methods with 6-31+G(d,p) basis set. The electronic dipole moment (μ) and the first hyperpolarizability (β) value of the investigate molecule computed show that the ADP molecule might have microscopic nonlinear optical (NLO) behavior with non-zero values. The calculated HOMO and LUMO energies show that charge transfer occurs in the molecule. Moreover, natural bond orbital analysis (NBO) performed using NBO 3.1 program provides valuable information about various intermolecular interactions that are responsible for its bioactivity.

2 Experimental Details

The pure compound 1-amino-2,6-dimethylpiperidine was purchased from Lancaster chemical company U K, and used as such without any further purification. The room temperature Fourier transform infrared (FTIR) spectrum of the title molecule was recorded in the region 4000-400 cm^{-1} at a resolution of ±1 cm^{-1} using a BRUKER IFS 66V FTIR spectrophotometer equipped with a cooled MCT detector. Boxcar apodization was used for the 250 averaged interferograms collected for both the samples and background. The FT-Raman spectrum was recorded on a computer interfaced BRUKER IFS model interferometer, equipped with FRA 106 FT-Raman accessory in the 3500-50 cm^{-1} stokes region, using the 1064 nm line of Nd:YAG laser for excitation operating

*Corresponding author (E-mail: sa75kumar@yahoo.co.in)

at 200 mW power. The reported wave numbers are believed to be accurate within ±1 cm^{-1}.

The entire calculations were performed at density functional theory (DFT) and Hartree-Fock (HF) levels using GAUSSIAN-09W program package[21], invoking gradient geometry optimization[22]. The basis set 6-31+G (d,p) was used as a effectively levels to study fairly large molecule. Based on these points, the density functional three parameter hybrid model (DFT/B3LYP) at the 6-31+G(d, p) basis set level with an *ab initio* HF method was adopted to calculate the properties of studied molecule. In this study, the DFT approach (B3LYP) has been utilized for the computation of molecular structure, vibrational frequencies and energies of optimized structures. Finally, the calculated normal mode vibrational frequencies provide thermodynamic properties also through the principal of statistical mechanics. By combining the result GAUSSVIEW program[23] with symmetry considerations vibrational frequency assignments were made with a high degree of accuracy. Transformation of the force field and subsequent normal coordinate analysis including the least square refinement of the scale factors, calculation of the total energy distribution (TED) and the predictions of IR and Raman intensities were done on a PC with the MOLVIB program (version 7.0-G77) written by Sundius[24]. The Raman intensities (S_i) calculated with GAUSSIAN-09W program have been suitably adjusted by the scaling procedure with MOLIVB and subsequently converted to relative Raman intensities (I_i) using the following relationship derived from the basis theory of Raman scattering[25-27]:

$$I_i = \frac{f(\nu_0 - \nu_i)^4 Si}{\nu_i \left[1 - \exp\frac{-hc\nu_i}{kT}\right]} \quad \ldots (1)$$

where, ν_0 is the exciting frequency (in cm^{-1}), ν_i is the vibrational wave number of the i^{th} mode h, c, k are universal constants, and f is a suitably chosen common scaling factors for all the peak intensities.

3 Results and Discussion

3.1 Molecular geometry

The optimized molecular structure of ADP obtained from GAUSSIAN 09W is shown in Fig. 1. The optimized geometrical parameters obtain by the large basis set calculations for ADP is presented in Table 1. Detailed description of vibrational modes can

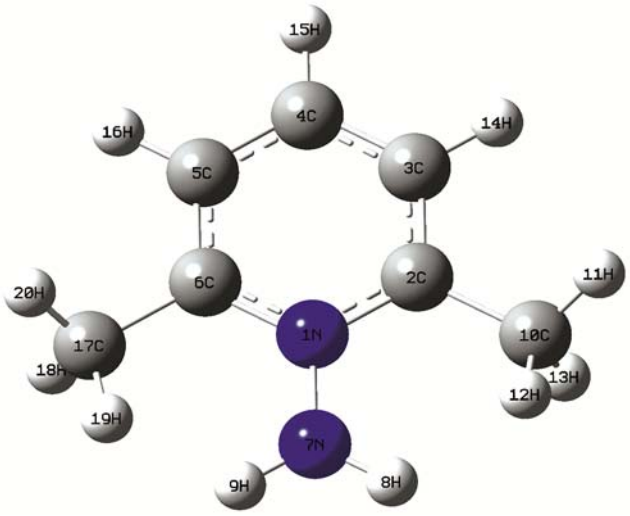

Fig. 1 – Molecular structure of 1-amino-2,6-dimethyl piperidine.

be given by means of normal coordinate analysis (NCA). For this purpose the full set of 69 standard internal coordinates (containing 15 redundancies) for ADP is given in Table 2. From these, a non-redundant set of local symmetry coordinates were constructed by suitable linear combinations of internal coordinates following the recommendations of Fogarasi and Pulay[24,28] are summarized in Table 3. The theoretically calculated DFT force fields were transformed to this latter set of vibrational coordinates and used in subsequent calculations.

3.2 Vibrational spectra

The molecular structure of ADP belongs to C_1 point group symmetry. For C_1 symmetry there would not be any relevant distribution. The molecule consists of 20 atoms and expected to have 54 normal modes of vibrations of the same *A* species under C_1 symmetry.

$\boxed{3N-6}$ = 37 A' (in-plane) + 17 A" (out-of-plane)

The detailed vibrational assignments of fundamental modes of ADP along with the observed and calculated frequencies and normal mode descriptions (characterized by TED) are reported in Table 4. The FTIR and FT-Raman spectra are shown in Figs 2 and 3, respectively.

3.2.1 C-H vibrations

Heteroaromatic structure shows the presence of C-H stretching vibration in the region 3100-3000 cm^{-1} which is the characteristic region for the identification of such C-H stretching vibrations[29]. These vibrations

Table 1 — Optimized geometrical parameters of 1- amino- 2,6-dimethylpiperidine obtained by HF/6-31+G(d,p) and B3LYP /6-31G+(d,p) density functional theory calculations

Bond length	Value (Å)		Bond angle	Value (°)		Dihedral angle	Value (°)	
	HF/ 6-31G+(d,p)	B3LYP/ 6-31G+(d,p)		HF/ 6-31G+(d,p)	B3LYP/ 6-31G+(d,p)		HF/ 6-31G+(d,p)	B3LYP/ 6-31G+(d,p)
N1-C2	1.4164	1.4167	C4-C3-H14	120.018	120.142	C6-N1-C2-C3	0.2868	1.4274
N1-C6	1.4179	1.4231	C3-C4-C5	117.774	117.500	C6-N1-C2-C10	176.352	117.699
N1-N7	1.405	1.4246	C3-C4-H15	121.141	121.252	N7-N1-C2-C3	143.118	150.711
C2-C3	1.3703	1.372	C5-C4-H15	121.071	121.245	N7-N1-C2-C10	-40.815	-33.017
C2-C10	1.5011	1.5003	C4-C5-C6	121.305	121.954	C2-N1-C6-C5	-0.051	-1.1168
C3-C4	1.4158	1.4173	C4-C5-H16	120.164	120.185	C2-N1-C6-C17	-174.575	-175.03
C3-H14	1.0753	1.086	C6-C5-H16	118.506	117.844	N7-N1-C6-C5	-141.564	-149.15
C4-C5	1.413	1.4108	N1-C6-C5	120.396	119.401	N7-N1-C6-C17	43.911	36.933
C4-H15	1.0731	1.0833	N1-C6-C17	116.414	116.866	C2-N1-N7-H8	-96.77	-99.819
C5-C6	1.373	1.3751	C5-C6-C17	122.947	123.43	C2-N1-N7-H9	141.082	140.724
C5-H16	1.0756	1.0866	N1-N7-H8	111.279	110.042	C6-N1-N7-H8	46.762	49.839
C6-C17	1.5029	1.5021	N1-N7-H9	110.10	109.190	C6-N1-N7-H9	-75.377	-69.615
N7-H8	1.003	1.0235	H8-N7-H9	109.924	108.883	N1-C2-C3-C4	-1.283-	-1.663
N7-H9	0.997	1.0148	C2-C10-H11	109.768	109.550	N1-C2-C3-H14	177.294	177.22
C10-H11	1.0838	1.0932	C2-C10-H12	110.443	110.959	C10-C2-C3-C4	-177.066	-177.67
C10-H12	1.0864	1.0976	C2-C10-H13	111.980	112.3283	C10-C2-C3-H14	1.508	1.2134
C10-H13	1.0831	1.0941	H11-C10-H12	108.575	108.626	N1-C2-C10-H11	-169.998	-172.03
C17-H18	1.0829	1.0927	H11-C10-H13	108.745	108.757	N1-C2-C10-H12	-50.314	-52.1046
C17-H19	1.0862	1.0969	H12-C10-H13	107.230	106.501	N1-C2-C10-H13	-69.116	66.9827
C17-H20	1.088	1.1004	C6-C17-H18	109.951	109.574	C3-C2-C10-H11	5.937	4.0634
			C6-C17-H 19	112.865	113.513	C3-C2-C10-H12	125.621	123.935
			C6-C17-H20	110.645	111.340	C-3-C2-C10-H13	-114.948	-116.916
			H18-C17-H19	107.537	107.329	C2-C3-C4-C5	1.9738	1.5322
			H18-C17-H20	108.087	107.747	C2-C3-C4-H15	-179.285	-178.87
			H19-C 17-H20	107.581	107.093	H14-C3-C4-C5	-176.568	-177.32

*For numbering of atoms refer to Fig. 1

Table 2 — Definition of internal coordinates of 1-amino-2, 6-dimethylpiperidine

Number (*i*)	Symbol	Type	Definition[a]
Stretching			
1-3	R_i	C-H	C_3 - H_{14}, C_4- H_{15},C_5- H_{16}
4-9	r_i	C-C	C_2 - C_3, C_3 - C_4, C_4 - C_5, C_5 - C_6, C_2 - C_{10},C_6 - C_{17}
10	S_i	N-N	N_1- N_7
11-12	q_i	C-N	C_2-N_1, C_6 -N_1
13-18	P_i	C-H_3methyl	C_{10} - H_{11}, C_{10}- H_{12},C_{10}- H_{13},C_{17} - H_{18},C_{17}- H_{19}, C_{17}- H_{20}
19,20	Q_i	NH_2	N_7-H_8,N_7-H_9
In-plane bending			
21-26	α_i	ring	N_1 - C_2 - C_3, C_2 - C_3 - C_4, C_3 - C_4 - C_5, C_4 - C_5 - C_6, C_5 - C_6 -N_1, C_6 - N_1 - C_2
27-32	β_i	C-C-H	C_2-C_3-H_{14},C_4-C_3-H_{14},C_3-C_4-H_{15},C_5-C_4-H_{15},C_6-C_5-H_{16},C_4-C_5-H_{16}
33-38	λ_i	C-C-Hmethyl	C_2-C_{10}-H_{13},C_2-C_{10}-H_{14},C_2-C_{10}-H_{15},C_6-C_{17}-H_{18},C_6-C_{17}-H_{19},C_6-C_{17}-H_{20}
39- 44	p_i	H-C-H	H_{13}-C_{10}-H_{12},H_{13}-C_{10}-H_{11},H_{12}-C_{10}-H_{11},H_{18}-C_{17}-H_{19},
		methyl	H_{18}-C_{17}-H_{20} ,H_{19}-C_{17}-H_{20}
45-46	Z_i	N-N-C	N_7-N_1-C_2,N_7-N_1-C_6
47,48	b_i	N-N-H	N_1-N_7-H_8,N_1-N_7-H_9
49	X_i	N-H-H	N_7-H_8-H_9
50-53	M_i	N-C-C	N_1-C_2-C_{10},N_1-C_2-C_3,N_1-C_6-C_{17},N_1-C_6-C_5
Out-of-plane bending			
54-56	ψ_i	C-H	H_{14}-C_3-C_2-C_4, H_{15}-C_4-C_5-C_3,H_{16}-C_5-C_6-C_4
57,58	ρ_i	N-H	N_7-N_1-C_2-C_6 ,N_1-N_7-H_9-H_8
59,60	χ_i	C-C	C_{10}-C_2-C_3-N_1 ,C_{17}-C_6-C_5-N_1
Torsion			
61-66	τ_i	t Ring	N_1 - C_2 - C_3 - C_4, C_2 - C_3 - C_4 - C_5, C_3 - C_4 - C_5 - C_6, C_4 - C_5 - C_6 - N_1, C_5 - C_6 - N_1 - C_2, C_6 - N_1 - C_2 - C_3
67	τ_i	t C-CH_3	(N_1 ,C_5)-C_6-C_{17}-(H_{18} ,H_{19},H_{20})
68	τ_i	t C-CH_3	(N_1,C_3)- C_2 - C_{10} – (H_{11},H_{12},H_{13})
69	τ_i	t N-NH_2	N_1-N_7-H_8-H_9

[a]For numbering of atoms refer to Fig. 1.

are not found to be affected due to the nature and position of the substituent. Accordingly, in the present study, the band identified at 3100 and 3000 cm^{-1} in FT-IR and 3150 cm^{-1} in FT-Raman spectrum has been designated to C-H stretching vibration and the corresponding force constant contribute 94% to the TED. The C-H in-plane-bending vibrations usually occur in the region 1390-990 cm^{-1} and are very useful for characterization purposes. Substitution patterns on the ring can be judged from the out-of-plane bending of the ring C-H in the region 900-675 cm^{-1} and these bands are highly informative[30]. Therefore, the FT-IR band observed at 1295, 1288 cm^{-1} and the Raman band observed at 1278 cm^{-1} have been assigned to, C-H in-plane-bending mode of ADP. The C-H out-of-plane bending modes are observed at 855 cm^{-1} in IR and in Raman 881, 860 cm^{-1} for title compound.

Table 3 — Definition of local symmetry coordinates of 1-amino-2, 6-dimethylpiperidine

Number (*i*)	Type	Definition[b]
1-3	C H	R_1, R_2, R_3
4-9	CC	$r_4, r_5, r_6, r_7, r_8, r_9$
10	NN	S_{10}
11,12	CN	q_{11}, q_{12}
13,14	CH_3 ss	$(p_{13} + p_{14} + p_{15})/\sqrt{3}$, $(p_{16} + p_{17} + p_{18})/\sqrt{3}$
15-16	CH_3 ass	$(2p_{13} + p_{14} + p_{15})/\sqrt{6}$, $(2p_{16} + p_{17} + p_{18})/\sqrt{6}$
17-18	CH_3 ops	$(p_{14} - p_{15})/\sqrt{6}$, $(p_{17} - p_{18})/\sqrt{6}$
19	NH_2ss	$(Q_{19} + Q_{20})/\sqrt{2}$
20	NH_2ips	$(Q_{19} - Q_{20})/\sqrt{2}$
21	R trigd	$(\alpha_{21} - \alpha_{22} + \alpha_{23} - \alpha_{24} + \alpha_{25} - \alpha_{26})/\sqrt{6}$
22	R symd	$(-\alpha_{21} - \alpha_{22} + 2\alpha_{23} - \alpha_{24} - \alpha_{25} + 2\alpha_{26})/\sqrt{12}$
23	R asymd	$(\alpha_{21} - \alpha_{22} + \alpha_{24} - \alpha_{25})/\sqrt{2}$
24-26	b C H	$(\beta_{27} - \beta_{28})/\sqrt{2}$, $(\beta_{29} - \beta_{30})/\sqrt{2}$, $(\beta_{31} - \beta_{32})/\sqrt{2}$
27,28	CH_3 sb	$(-\lambda_{33} - \lambda_{34} - \lambda_{35} + \lambda_{36} + \lambda_{37} + \lambda_{38})/\sqrt{2}$, $(-p_{39} - p_{40} - p_{41} + p_{42} + p_{43} + p_{44})/\sqrt{2}$
29,30	CH_3 ipb	$(2\lambda_{38} - \lambda_{37} - \lambda_{36})/\sqrt{6}$, $(2p_{44} - p_{43} - p_{42})/\sqrt{6}$
31,32	CH_3 opb	$(-\lambda_{36} + \lambda_{37})/\sqrt{2}$ $(-p_{42} + p_{43})/\sqrt{2}$
33,34	CH_3 ipr	$(-\lambda_{35} - \lambda_{34} + 2\lambda_{33})/\sqrt{6}$, $(-p_{41} - p_{40} + 2p_{39})/\sqrt{6}$
35,36	CH_3 opr	$(-\lambda_{34} + \lambda_{35})/\sqrt{2}$, $(-p_{40} + p_{41})/\sqrt{2}$
37	b N C	$(Z_{45} - Z_{46})/\sqrt{2}$
38	b N H	$(b_{47} - b_{48})/\sqrt{2}$
39	b HH	X_{49}
40,41	b CC	$(M_{50} - M_{51})/\sqrt{2}$, $(M_{52} - M_{53})/\sqrt{2}$
42-44	ω C H	$\psi_{54}, \psi_{55}, \psi_{56}$
45,46	ω NH	ρ_{57}, ρ_{58}
47,48	ω CC	χ_{59}, χ_{60}
49	tRtrigd	$(\tau_{61} - \tau_{62} + \tau_{63} - \tau_{64} + \tau_{65} - \tau_{66})/\sqrt{6}$
50	tRsymd	$(\tau_{61} - \tau_{63} + \tau_{64} - \tau_{66})/\sqrt{2}$
51	tRasymd	$(-\tau_{61} + 2\tau_{62} - \tau_{63} - \tau_{64} + 2\tau_{65} - \tau_{66})/\sqrt{12}$
52,54	τC-CH_3	τ_{67}, τ_{68}
54	τ N-NH_2	τ_{69}

[b]The internal coordinates used here are defined in Table 2.

3.2.2 C-C vibrations

The bands between 1400-1650 cm^{-1} in aromatic derivatives are due to C-C stretching vibrations[31]. Therefore, the FTIR and FT-Raman bands are found at 1727, 1695, 1665 cm^{-1} and 1702, 1671, 1656 cm^{-1} have been assigned to C-C stretching vibrations of ADP, respectively. Also, the ring modes are affected by the substitutions in the aromatic ring of the title compound. Accordingly, in the present study, both FTIR and FT-Raman bands observed at 832 and 743 cm^{-1} have been assigned to ring in-plane bending modes of ADP, respectively. The ring out-of-plane bending modes of ADP are also listed in Table 4. The reductions in the frequencies of these modes are due to the change in force constant and the vibrations of functional groups present in the molecule[32].

3.2.3 C-N vibrations

The identification of C-N stretching vibration is a difficult task, since the mixing of vibrations is possible in this region. However, with the help of force field calculations, the C-N vibrations are identified and assigned in this study. The bands are observed at 1489 and 1477 cm^{-1} in FTIR and at 1488, 1476 cm^{-1} in FT-Raman spectrum for the title compound. These assignments are also supported by the literature[33].

3.2.4 NH_2 vibrations

The molecule under consideration posses NH_2 group and hence six internal modes of vibration are possible such as symmetric stretching, asymmetric stretching, scissoring, rocking, wagging and torsional mode. The frequency of asymmetric vibration is higher than that of symmetric one. The frequencies of amino group in the region 3500-3300 cm^{-1} for NH stretching, 1700-1600 cm^{-1} for scissoring and 1150-900 cm^{-1} for rocking deformation[34]. In the present study, the asymmetric and symmetric modes of NH_2 group are assigned at 3347 cm^{-1} (FTIR) and 3320 cm^{-1}

Table 4 — The observed FTIR, FT-Raman and calculated (unscaled and scaled) frequencies (cm^{-1}), IR intensity (km mol^{-1}), Raman activity (A^0 amu^{-1}) and force constant (m dyne A^0) and probable assignments (Characterized by TED) of 1-amino-2,6-dimethylpiperidine using HF6-31+G(d, p) and B3LYP /6-31+G(d, p) calculations

Symmetry species C_1	Observed frequencies (cm^{-1})		Calculated frequencies (cm^{-1}) (Unscaled)		Scaling frequency (cm^{-1})		Force constant (mDyne/A)		IR intensity (KM/Mole)		Raman activity (A^4/amu)		Assignment (% TED)
	FTIR	FT-Raman	HF	B3LYP	HF	B3LYP	HF	B3LYP	HF	B3LYP	HF	B3LYP	
A'	3347vw	-	3847	3578	3358	3350	9.5269	8.1663	8.9511	14.204	47.169	51.076	NH_2ass(99)
A'	-	3320vw	3706	3400	3330	3326	8.5217	7.1952	5.0335	45.269	123.37	556.42	NH_2ss (98)
A'	-	3150vw	3374	3223	3157	3154	7.3450	6.6955	22.902	11.340	195.05	201.45	νCH(97)
A'	3100s	-	3352	3190	3109	3102	7.2261	6.5353	30.062	22.907	62.172	91.059	νCH(96)
A'	3000vs	-	3345	3183	3009	3003	7.1741	6.5014	2.3493	11.704	78.381	100.70	νCH(95)
A'	2962ms	-	3269	3127	2973	2963	6.9418	6.3483	27.605	15.105	55.813	59.226	CH_3ss(64) , νCC(25), tRasymd(11)
A'	-	2938vs	3268	3126	2948	2940	6.9266	6.3122	18.999	12.121	64.959	61.698	CH_3ss(60), νCC(22), tRsymd(13)
A'	2930s	-	3247	3090	2939	2932	6.8189	6.1490	27.225	14.905	72.525	80.589	CH_3ips(59), νCH(23), tRtrigd(12)
A'	-	2886s	3217	3052	2899	2890	6.7113	5.9980	29.531	16.733	69.849	64.899	CH_3ips(53), νCH(26), bCC(16)
A'	2860w	-	3185	3030	2876	2867	6.2179	5.6406	44.375	50.560	162.98	295.60	CH_3ops(52) , νCH(23), bCC(11)
A'	-	2801s	3169	3001	2810	2804	6.1616	5.5628	46.673	68.843	145.27	333.76	CH_3ops (57), NH_2rock(24)
A'	1727w	-	1822	1673	1739	1730	2.1323	1.9183	23.677	11.646	4.3747	18.897	νCC(83), νNN(11)
A'	-	1702w	1691	1653	1711	1705	6.2697	6.9079	3.1232	10.333	31.195	151.74	νCC (57), CH_3ips(30), ωCH(12)
A'	1695vw	-	1636	1549	1709	1700	2.3169	3.8042	0.1211	1.0677	6.6351	1.4962	νCC(55) ,CH_3ips(25), ωCH(19)
A'	-	1671w	1617	1500	1686	1675	1.7591	1.4587	3.3402	3.5496	3.8378	10.361	νCC(57), CH_3sb(29) ,bNN(14)
A'	1665s	-	1602	1488	1679	1670	1.6003	1.4988	9.6728	10.144	9.9844	13.806	νCC(44), CH_3sb(35)
A'	-	1656ms	1598	1480	1668	1660	2.2588	1.3560	9.6513	9.5212	1.1191	11.890	νCC(53), bCH(26), CH_3ipr(13)
A'	1649vs	-	1594	1471	1659	1652	1.5792	1.3329	6.5612	8.8125	8.7030	8.7853	NH_2siss (52),bCH (28),Rasymd(18)
A'	1489ms	1488w	1552	1426	1510	1492	1.8614	1.6544	0.9442	2.8404	2.9218	15.892	νCN(56), bCH(21),Rsymd(13)
A'	1477s	1476vw	1549	1424	1497	1482	1.9653	1.6032	5.5178	4.2989	6.0362	10.873	νCN(44), bCH(27),Rtrigd(21)
A'	1463vs	-	1520	1403	1474	1469	3.2238	2.8294	10.549	8.8907	5.6953	55.996	CH_3ipb(43), bCH(30), NH_2rock(21)
A'	-	1459w	1509	1397	1469	1463	2.9733	2.3430	7.2223	4.3799	20.030	77.209	CH_3ipb(40), bCH(31),bNN(22)
A'	1380s	-	1440	1336	1396	1383	3.6601	2.3750	29.643	20.795	6.4521	6.498	CH_3sb(39), νCC(25), NH_2twist(17)
A'	-	1373w	1414	1301	1382	1375	4.4324	1.2650	21.002	20.201	2.4245	1.496	CH_3sb(47) , νCC(27), bCH(17)
A'	1295ms	-	1348	1255	1308	1298	2.4076	2.2147	2.7355	2.8361	3.6475	2.8361	bCH(46) , νCC(34),CH_3ips(13)
A'	1288s	-	1337	1252	1297	1290	4.0298	3.6085	7.3325	3.4970	2.6998	3.4970	bCH (40), νCC(33),CH_3ips(20)
A'	-	1278vw	1284	1178	1289	1280	4.1556	2.6905	16.885	16.406	12.850	16.406	bCH (41), NH_2siss (36), CH_3sb(19)
A'	1258ms	-	1194	1124	1266	1260	1.2092	1.0660	0.3855	2.2594	0.0977	4.0482	νNN(52),bCN(35),CH_3sb(13)
A'	-	1200ms	1135	1076	1220	1205	1.1575	1.1097	1.4365	19.960	0.5762	4.5166	CH_3opb (47), bCN(30),CC (18)
A'	-	1193ms	1134	1055	1209	1197	1.1242	0.9486	1.4743	1.0347	0.4698	0.3895	CH_3opb (46) ωCC(33) CN(12)
A'	-	1170ms	1131	1051	1189	1174	1.0785	0.9811	0.5629	1.0466	0.4154	1.0988	NH_2rock(45), ωCC(22),CC (18)
A'	1120s	-	1122	1044	1138	1124	1.1359	1.0543	8.5592	6.0788	1.0129	3.9460	Rasymd(40), ωNN(31),CC(15)
A'	1110s	-	1057	999	1125	1114	1.4427	1.0666	2.7364	6.4258	6.7235	13.419	Rsymd(43), NH_2twist(30),bCC(17)
A'	-	1100w	1023	944	1110	1104	1.0116	1.0688	96.437	42.334	1.5114	2.9574	Rtrigd(48), tCH_3(31), bCC(14)
A'	990s	-	934	890	1000	992	0.6988	0.6002	8.8528	10.313	0.2242	0.5486	CH_3ipr(49) tCH_3 (39) bCC(11)
A'	963ms	-	933	882	975	965	0.6801	0.5942	23.171	6.5368	0.2376	0.1388	CH_3ipr (44), NH_2wag(25)
A'	-	958s	902	851	987	961	0.9329	0.7848	36.090	36.930	0.6166	2.5215	bNN(48), bCC(34)
A"	940vs	-	871	800	965	943	2.1260	1.7689	17.698	21.363	0.3422	1.8071	CH_3opr (42),bCC(33),bCN(14)
A"	901s	-	708	669	937	906	0.4409	1.1858	44.838	8.936	2.1220	17.344	CH_3opr (35) ,ωNN(20)
A"	-	881ms	697	658	900	886	0.8453	0.3127	22.265	52.830	9.4913	11.122	ωCH (47),bNN(28)
A"	-	860ms	635	626	886	868	0.9149	0.9315	6.7243	10.964	0.9158	0.9106	ωCH (44), ωCH (35)
A"	855ms	-	578	550	868	860	0.8999	0.8463	3.8147	3.5573	4.4393	7.5705	ωCH (43),CH_3ops (22)
A"	850ms	-	538	514	860	855	0.6305	0.5660	4.0928	3.7626	0.5359	1.2592	NH_2wag(45) ,CH_3ss(34)
A"	832s	832s	508	477	843	834	0.8505	0.7378	2.4743	2.0818	5.1860	11.8246	bCC(44) CH_3ips(22)
A"	743vs	743vs	478	463	753	745	0.3692	0.3631	4.3098	3.9612	0.1710	1.5821	bCC(41) ,CH_3ips(25)
A"	706s	-	422	388	717	709	0.6567	0.2880	7.3141	13.904	0.2935	2.2638	tRtrigd(46),CH_3opr(22)
A"	-	693ms	391	361	709	699	0.1495	0.2005	26.566	7.7729	0.8703	0.4134	tRsymd(43) ,NH_2wag(21)
A"	-	688s	369	321	698	693	0.1556	0.0699	11.096	27.152	0.7666	6.3028	tRasymd(48), bNN(29)
A"	-	456ms	318	304	473	460	0.1529	0.1570	1.7443	1.3716	0.9149	1.6497	ωCC(54),ωCH (19)
A"	450s	-	340	236	463	453	0.0612	0.0534	0.1295	0.2484	0.9723	2.2497	ωCC(53),ωCH (14)
A"	-	424w	230	217	433	427	0.0691	0.0601	14.138	13.329	1.2607	2.0365	ωNN(52),ωCH (13)
A"	-	310vw	189	189	323	314	0.0280	0.0297	2.2160	5.1134	0.4629	1.5736	NH_2twist(55)
A"	-	170w	165	164	179	175	0.0213	0.0218	0.2325	0.7026	0.0304	0.3035	t CH_3 (37)
A"	103ms	-	78	77	120	108	0.0125	0.0121	2.0057	2.0237	0.6700	1.0238	tCH_3 (32)

*Abbreviations: ν - stretching; b - in-plane bending; ω - out-of-plane bending; asymd - asymmetric; symd - symmetric; t - torsion; trig - trigonal; w - weak; vw - very weak; vs - very strong; s - strong; ms - medium strong; ss - symmetric stretching; ass - asymmetric stretching; ips - in-plane stretching ops - out-of-plane stretching; sb - symmetric bending; ipr - in-plane rocking; opr - out-of-plane rocking; opb - out-of-plane bending

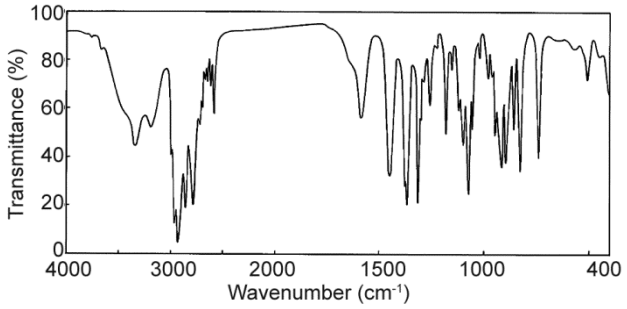

Fig. 2 — FTIR spectrum of 1-amino-2,6-dimethylpiperidine.

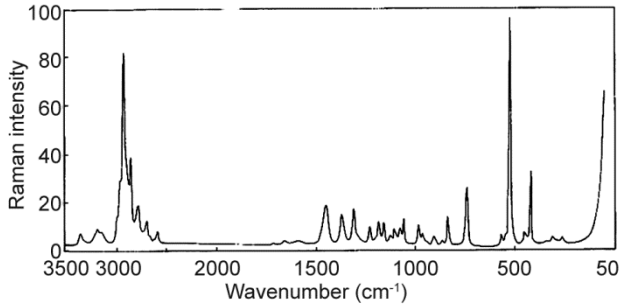

Fig. 3 — FT Raman spectrum of 1-amino-2,6-dimethylpiperidine.

(FT-Raman), respectively. The band observed at 1649 cm^{-1} in FTIR spectrum is assigned to NH_2 scissoring mode. The rocking, wagging, twisting deformation vibrations of NH_2 contribute to several normal modes in the low frequency region. The band observed at 1170 cm^{-1} in raman is assigned to NH_2 rocking vibrations and the FTIR band observed at 850 cm^{-1} is assigned to NH_2 wagging modes, and the band observed at 310 cm^{-1} in raman is assigned to NH_2 twisting modes[35].

3.2.5 CH_3 group vibrations

The title molecule ADP, under consideration possesses two CH_3 groups in second and sixth position of the ring. For the assignments of CH_3 group frequencies one can expected that nine fundamentals can be associated to each CH_3 group, namely three stretching, three bending, two rocking modes and a single torsional mode describe the motion of methyl group. The above modes are defined in Table 4. The CH_3 symmetric stretching frequency are identified at 2962 cm^{-1} in FTIR and in FT-Raman 2938 cm^{-1} and CH_3 in-plane stretching vibrations are identified at 2930 cm^{-1} in IR and 2938, 2886 cm^{-1} in raman spectra. The CH_3 symmetric bending and CH_3 in-plane bending frequencies are attributed at 1380 cm^{-1} and 1463 cm^{-1}, in IR, 1373 cm^{-1} and 1459 cm^{-1} in raman spectra respectively. These assignments are supported by literature[36]. The in-plane rocking and out-of-plane rocking modes of CH_3 group are found at 990, 963 cm^{-1} and 940, 901 cm^{-1} in IR spectra, respectively. The bands obtained at 2860 cm^{-1} in IR, 2801 cm^{-1} and 1200, 1193 cm^{-1} in Raman are assigned to CH_3 out-of-plane stretching and CH_3 out-of-plane bending modes, respectively. The assignment of the bands at 103 cm^{-1} in IR and 170 cm^{-1} in Raman are attributed to methyl twisting mode.

4 NMR Spectral Analyses

NMR spectroscopy is a powerful technique that can provide detailed information on the topology, dynamics and three-dimensional structure of molecules in solid state and solution. This technique used to obtain physical, chemical, electronic and structural information about molecules due to their chemical shift, on the resonant frequencies of the nuclei present in the molecule. GIAO/DFT (Gauge including atomic orbital/density functional theory) approach is widely used as for the calculations of chemical shifts for different type of molecules[37-40]. ^{13}C-NMR chemical shift is one of the important tools in determining the presence or absence of particular atom in a particular position of a molecular system. In a molecule, shielding of atom like carbon is greatly affected by neighboring bonded atoms and similar bonded atoms give different shielding values in different environments. By adopting the procedure recommended the chemical shift values for carbon atom have been studied. The NMR calculation were carried out at B3LYP/6-31+G(d,p) levels of theory in the gas phase. In this work the chemical shift (δ) for carbon atoms presented in the ADP in gas phase has been studied and theoretical ^{13}C, ^{1}H-NMR isotropic shielding of carbon and Hydrogen atom and NMR shielding surface as shown in Fig. 4. The corresponding values are shown in Table 5. The result shows that the range ^{13}C NMR chemical shift of the typical organic molecule usually[41,42], the accuracy ensures reliable interpretation of spectroscopic parameters. It is true from the above literature value in our present study, that the title molecule (ADP) also shows that same. The molecule structure of the title molecule shows that the two CH_3 are present in two different positions. The presence of electronegative atom attracts all electron clouds of carbon atom towards the CH_3 atom, which leads to deshielding of carbon atom and the net result is increase in chemical shift values.

So, the CH_3 atoms show electronegative property (they attract the other atom towards), but the chemical

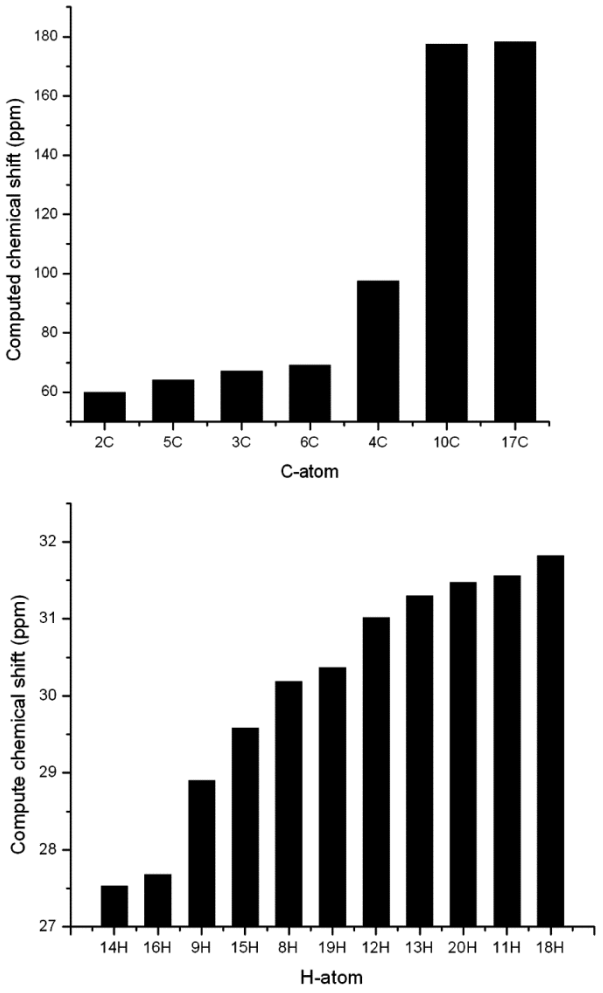

Fig. 4 — Prediction of ^{13}C, ^{1}H chemical shift value of 1-amino-2,6-dimethylpiperidine.

shift of C_2, C_3, C_4, seems to be (C_2=59.94; C_3= 67.17; C_4=97.47; C_5=64.09; C_6=69.18 ppm) by B3LYP/6-31+G(d,p) method same for other carbon atoms but in N_1 the chemical shift is higher value, i.e., 178.28 ppm using B3LYP/6-31+G(d,p) methods. The H atom is the smallest of all atoms and mostly localized on the periphery of molecules. Therefore their chemical shifts would be more susceptible to intermolecular interactions in the aqueous solution as compared to that for other heavier atoms. The H_{14}, H_{15} and H_{16} are expected to give rise to NMR signals in (27.53-30.19) ppm range. Another important aspect is that, hydrogen attached or nearly electron-withdrawing atom or group can decrease the shielding and more the resonance of attached proton towards to a higher frequency. By contrast electron donating atom or group increase the shielding and moves the resonance towards to a lower frequency. In this study, the chemical shift obtained and calculated for the hydrogen atoms of methyl groups are quite low. It is also true from the above literature[43] data in our present study the methyl protons at C_{10}, C_{17} appears as a singlet with three proton integral at 177.46,178.28 ppm. On the other hand the isotropic chemical shifts for the carbon atoms are shown in Table 6. The relationship between the experimental chemical shift and computed GIAO/ B3LYP/6-31+G(d, p) levels for ^{13}C are shown in Fig. 5.

5 First Hyperpolarizability

The potential application of the title compound in the field of nonlinear optics demands, the investigation of its structural and bonding features contribution to the hyperpolarizability enhancement, by analysing the vibrational modes using IR and Raman spectroscopy. Many organic molecules, containing conjugated π electrons are characterized by large values of molecular first hyper polarizabilities, were analysed by means of vibration spectroscopy[44,45]. In most of the cases, even in the absence of inversion symmetry, the strongest band in the Raman spectrum is weak in the IR spectrum and vice-versa.

But the intramolecular charge from the donor to acceptor group through a π-bond conjugated path can induce large variations of the molecular dipole moment and the molecular polarizability, making IR and raman activity strong at the same time. The experimental spectroscopic behavior described above is well accounted for a calculations in π conjugated systems that predict exceptionally infrared intensities for the same normal modes. The first hyperpolarizability (β) of this novel molecular system is calculated using the *ab initio* quantum mechanical method, based on the finite-field approach. In the presence of an applied electric field, the energy of a system is a function of the electric field. The first hyperpolarizability is a third-rank tensor that can be described by a 3×3×3 matrix. The 27 components of the 3D matrix can be reduced to 10 components due to the Kleinman symmetry[46]. The components of β are defined as the coefficients in the Taylor series expansion of the energy in the external electric field. When the electrical field is weak and homogeneous, this expansion becomes:

$$E = E_0 - \sum_i \mu_i F^i - \frac{1}{2}\sum_{ij} \alpha_{ij} F^i F^j - \frac{1}{6}\sum_{ijk} \beta_{ijk} F^i F^j F^k - \frac{1}{24}\sum_{ijkl} \nu_{ijkl} F^i F^j F^k F^l \quad \ldots (2)$$

Table 5 — Second order perturbation analysis of Fock matrix in NBO basis for ADP

Donor (*i*)	ED/e	Acceptor (*j*)	ED/e	[a]*E*(2)	[b]*E*(*j*)-*E*(*i*)	[c]*F*(*i*, *j*)
σN1-C2	0.9897	σ*N1-C6	0.0181	2.24	1.36	0.070
σN1-C6	0.8876	σ*N1-C2	0.1459	2.29	1.37	0.071
σ C2-C3	0.9904	σ*N1-N7	0.0168	2.41	0.98	0.061
σ C2-C10	0.9864	σ*N1-C6	0.0130	2.03	1.12	0.060
σ C5-H16	0.9907	σ*N1-C6	0.0181	2.53	1.04	0.065
σC17-H20	0.8343	σ*N7-H9	0.3771	2.51	1.04	0.065
π N1-C2		π* C5-C6	0.2434	14.04	0.37	0.092
π C5-C6	0.9899	n*C4	0.0181	26.71	0.19	0.101
π C5-C6	0.9886	π* N1-C2	0.0074	5.47	0.24	0.048
nC3	0.5412	n*C4	0.3771	207.43	0.05	0.140
nC3		π*N1-C2	0.2434	71.75	0.10	0.124
nN7	0.3771	π*N1-C2	0.1459	2.06	0.35	0.038
nN7	0.9735	σ *N1-C6	0.2434	1.98	0.86	0.052
n*C4	0.0168	π*C5-C6	0.0181	33.23	0.09	0.094
π*N1-C2		π*C5-C6	0.1459	35.03	0.04	0.073

[a]$E^{(2)}$ means energy of hyper-conjugative interactions (stabilization energy).
[b]Energy difference between donor and acceptor *i* and *j* NBO orbitals.
[c]$F(i,j)$ is the Fock matrix element between *i* and *j* NBO orbitals.

Table 6 — Experimental and theoretical chemical shifts of ADP in 13C NMR spectra [δ (ppm)]

Atom position	B3LYP/6-31+G(d,p)	Experimental[52]	Δ
N1	135.62		
C2	59.94	119.53	59.59
C3	67.14	128.87	61.73
C4	97.47	122.79	25.32
C5	64.09	127.68	63.59
C6	69.18	116.38	47.2
N7	198.06		
H8	30.37		
H9	29.58		
C10	177.46		
H11	31.50		
H12	31.04		
H13	31.05		
H14	27.53		
H15	30.19		
H16	27.68		
C17	178.28		
H18	31.82		
H19	31.02		
H20	31.47		

*$\Delta(\delta_{exp}-\delta_{the})$; difference between respective chemical shifts.

where E_0 is the energy of the unperturbed molecule; F^i is the field at the origin; and μ_i, α_{ij} β_{ijk} and ν_{ijkl} and are the components of dipole moment, polarizability, the first hyperpolarizabilities and second hyperpolarizibilities, respectively. The calculated total dipole moment (μ) and mean first hyperpolarizability (β) of ADP are 0.4069 Debye and 6.26605×10^{-30} esu, respectively, which is comparable with the reported values of similar derivatives. The large value of hyperpolarizibilities, β which is a measure of the

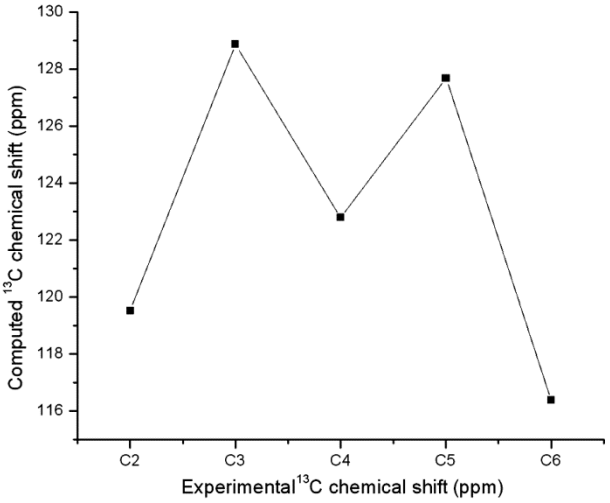

Fig. 5 — Computed NMR chemical shift value of 1-amino-2,6-dimethyl piperidine.

non-linear optical activity of the molecular system, is associated with the intramolecular charge transfer, resulting from the electron cloud movement through π conjugated frame work from electron donor to electron acceptor groups. The physical properties of these conjugated molecules are governed by the high degree of electronic charge delocalization along the charge transfer axis and by the low band gaps. So we conclude that the title compound is an attractive object for future studies of nonlinear optical properties.

6 Natural Bond Orbital Analyses

The NBO method demonstrates the bonding concepts like atomic charge, Lewis structure, bond type, hybridization, bond order, and charge transfer

and resonance weights. Natural bond orbital (NBO) analysis is a useful tool for understanding delocalisation of electron density from occupied Lewis-type (donor) NBOs to properly unoccupied non-Lewis type (acceptor) NBOs within the molecule. The stabilization of orbital interaction is proportional to the energy difference between interacting orbitals[47]. Therefore, the interaction having strongest stabilization takes place between effective donors and effective acceptors. This bonding-anti bonding interaction can be quantitatively described in terms of the NBO approach that is expressed by means of second–order perturbation interaction energy $E^{(2)}$. This energy represents the estimate of the off–diagonal NBO Fock matrix element. The stabilization energy $E^{(2)}$ associated with i (donor) $\rightarrow$ j (acceptor) delocalization is estimated from the second–order perturbation approach as given below:

$$E^{(2)} = \Delta E_{ij} = q_i \frac{F(i,j)^2}{\varepsilon_j - \varepsilon_i} \cdots \quad \ldots (3)$$

where q_i is the donor orbital occupancy, are ε_i and ε_j diagonal elements and $F(i, j)$ is the off diagonal NBO Fock matrix element. Natural bond orbital analysis provides an efficient method for studying intra and intermolecular bonding and interaction among bonds, and also provides a convenient basis for investigating charge transfer or conjugative interaction in molecular systems. Some electron donor orbital, acceptor orbital and the interacting stabilization energy resulted from the second-order micro-disturbance theory are reported[48,49]. The large the $E^{(2)}$ value the more intensive is the interaction between electron donors and electron acceptors, i.e., the more donating tendency from electron donors to electron acceptors and the greater the extent of conjugation of the whole system.

Delocalization of electron density between occupied Lewis-type (bond or lone pair) NBO orbitals and formally unoccupied (antibond or Rydgberg) non-Lewis NBO orbitals correspond to a stabilizing donor-acceptor interaction. NBO analysis has been performed on the ADP molecule at the DFT/B3LYP/6-31G+(d,p) level in order to elucidate, the intra-molecular, rehydridization and delocalization of electron density within the molecule. Maximum energy transfer from lone pair nC3 to n^*C4 (207.43 kj/mol), this investigation deeply mentioned the energy delocalization from the lone pair of the molecule to other part, which is listed in Table 5.

7 Frontier Molecular Orbital Analysis

The properties of the frontier molecular orbitals (FMOs) are very useful for physicists and chemists. The eigen values of the lowest unoccupied molecular orbital (LUMO) and the highest occupied molecular orbital (HOMO) and their energy gap (HOMO-LUMO gap, ΔE) reflect the chemical reactivity of the molecule. Recently, the energy gap between HOMO and LUMO has been used to prove the bioactivity from intra-molecular charge transfer[50,51] (ICT). The HOMO and LUMO pictures are shown in Fig. 6. It is found that the electron cloud distribution of HOMO is mainly localized on the benzene ring π-system and extended to the C4-C5, C2-N1 and N1-N7 bonds. Whereas, the electron cloud distribution of LUMO is eventually centralized on the NH_2 group of the heterocycles. The E_{HOMO} and E_{LUMO} are calculated to be -0.3250 a.u. and -0.1607 a.u., respectively. The HOMO-LUMO energy gap (ΔE) represents the lowest energy electronic transition. In the studied compound, the HOMO-LUMO energy gap of the studied compound is -0.1643 a.u.

HOMO energy= -0.3250 a.u.
LUMO energy= -0.1607 a.u.
HOMO-LUMO energy gap = -0.1643 a.u.

The calculated self- consistent field (SCF) energy of ADP is -382.826994 a.u. The HOMO and LUMO energy gap explains the fact that eventual charge transfer interaction is taking place within the molecule.

8 Conclusions

Based on the calculations *ab initio*/HF and density functional theory/B3LYP with 6-31+G(d,p), levels, complete vibrational properties of ADP have been investigated by FTIR and FT-Raman spectroscopies, respectively. A good correlation was found between the computed and experimental wave numbers. The calculated first hyperpolarizability was found to be 6.26605×10^{-30} esu. Simultaneous IR and raman activation of the heterocyclic ring modes provide evidence for the charge transfer interaction between the donor and the acceptor groups. Therefore, the assignments made at higher level of the theory with higher basis set with only reasonable deviations from the experimental values, seems to be correct. HOMO and LUMO energy gap explains the eventual charge transfer interactions taking place within the molecule. The lone pair electrons which provide stabilization to

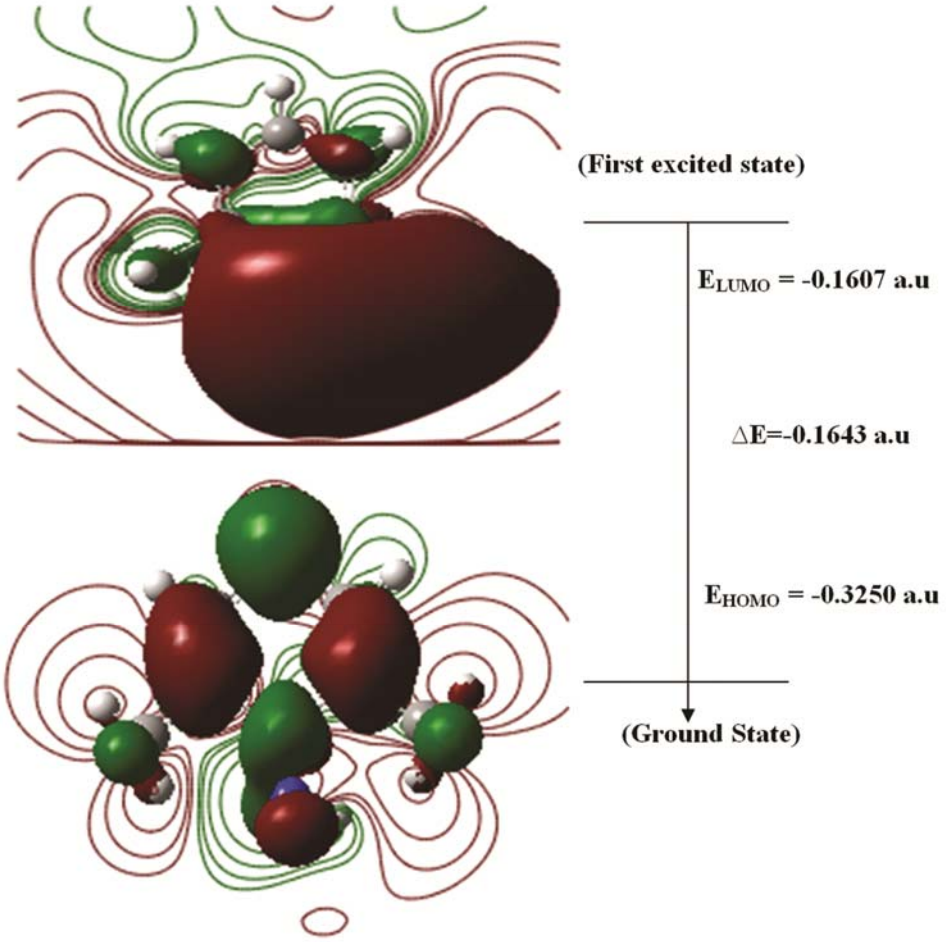

Fig. 6 — HOMO-LUMO plot of 1-amino-2,6-dimethylpiperidine.

the molecular structure enhance its bioactivity. This study demonstrates that scaled calculations are powerful approach for understanding the vibrational spectra of medium sized organic compounds.

References

1 Richardo G J, Juan B C, Mario R A, Roldan M & Peinado C R, *Fernando Spen*, 47 (1979) 168.
2 Jerom B R & Spencer K H, *Eur Pat Appl*, (1998) 277794.
3 Perumal R V, Adiraj M & Shanmugapandian P, *Indian drugs*, 38 (2001) 156.
4 Bochringer C F & Schochne G M B H, *Brit Pat Appl*, 866488 (1961).
5 Ganellin C R & SpickettR G, *J Med Chem*, 8 (1965) 619.
6 Nikolov M, Stefanora D & Chardanov D, *Act Nerv Super*, 16 (1974) 264.
7 Kathleen B, Jean-Peirre C & Andre H, *Eur Pat Appl Ep*, 169139 (1986).
8 Hagenbach R E & Gysin H, *Experientia*, 8 (1952) 184.
9 Heana B, Dobre V & Niculesucu-Duvaz I, *J Prakt Chem*, 327 (1985) 667.
10 Mobio I G, Soldatenkov A T, Fedrov V O, Ageev E A, Sergeeva N D, Lin S, Stashenko E E, Prostakov N S & Andreeva E I, *Khim Farm Zh*, 23 (1989) 421.
11 Gulluoglu M T, Erdogdu Y & Yurdakul S, *J Mol Struct*, 834 (2007) 540.
12 Erdogdu Y & Gluoglu M T, *Spectrochim Acta A*, 74 (2009) 162.
13 Pentin Yu A & Anisimova O S, *Opt Spectrosc*, 26 (1968) 35.
14 Hirokawa T, Kimura T, K. Ohno & Murata H, *Spectrochim Acta A*, 36 (1980) 329.
15 Marcotrigiano G, Meanbue L & Pellacani G C, *J Mol Struct*, 30 (1976) 85.
16 Okishi Y, Imai Y & Aida K, *J Inorg Nucl Chem*, 13 (1973) 101.
17 Titova T V & Anisimova O S, *Opt Spectrosc*, 23 (1967) 495.
18 Vedal D, Ellestad O, Klaboe P & Hagen G, *Spectrochim Acta A*, 32 (1976) 877.
19 Vayner E & Ball D W, *J Mol Struct*, 496 (2000) 175.
20 Sebastain S & Sundaraganesan N, *Spectrochim. Acta A*, 75 (2010) 941.
21 Frisch M J, Trucks G W & Schlegal H B, *Gaussian 09, Revision A 02*, (Gaussian, Inc: Wallingford CT), 2009.
22 Schiegal H B, *J Comput Chem*, 3 (1982) 214.
23 Frisch A, Nielson A B & Holder A J, *GAUSSVIEW User Manual*, (Gaussian Inc: Pittsburg, PA), 2000.
24 Sundius T, *J Mol Struct*, 218 (1990) 321.
25 Polavarapu P L, *J Phys Chem*, 94 (1990) 8106.
26 Keresztury G, Holly S, Varga J, Besenyei G, Wang A.Y, J & Durig J R, *Spectrochim Acta*, 49A (1993) 2007.

27 Keresztury G, Chalmers J M & Griffith P R, *Handbook of vibrational spectroscopy* Vol. 1, (John Wiley, New York) 2002

28 Fogarasi G, Zhou X, Taylor P W & Pulay P, *J Am Chem Soc*, 114 (1992) 8191.

29 Arivazhagan M, Sambathkumar K & Jeyavijayan S, *Indian J Pure Appl Phys*, 48 (2010) 716.

30 Arivazhagan M & Jeyavijayan S, *Indian J Pure Appl Phys*, 49 (2011) 516.

31 Sambathkumar K & Nithiyanantham S, *J Mater Sci: Mater Electron*, 28 (2017) 6529

32 Cecily Mary Glory D, Madivanane R & Sambathkumar K, *Elixir Comp Chem*, 89 (2015) 36730.

33 Kuppusamy S K, *Density functional theory studies of vibrational spectra, HOMO- LUMO, NBO and NLO analysis of some cyclic and heterocyclic compounds*, Bharathidasan University, Tiruchirappalli, 2014.

34 Kuppusamy S K, *Spectrochim Acta A*, 147 (2015) 51.

35 Sundaraganesan N, Dominic Joshua B, Rajamoorthy M & Gangadhar C H, *Indian J Pure Appl Phys*, 45 (2007) 969.

36 Arivazhagan M & Prabhakaran S, *Indian J Pure Appl Phys*, 50 (2012) 26.

37 Krushelnitsky A, Faizullin D & Reichert D, *Biopolymers*, 73(1) (2004) 1.

38 Osmialowski B, Kolehmainen E & Gawinencki R, *Magn Reson Chem*, 39 (2001) 334.

39 Marek R, Brus J, Tousk J, Kovacs L & Hockova D, *Magn Reson Chem*, 40 (2002) 353.

40 Meng Z & Carper W R, *J Mol Struct Theochem*, 588 (2002) 45.

41 Kalinowski H O, Berger S & Brawn S, *Cabon^{-13} chemical shifts in structure and sons,* (John Wiley. & Sons: Chichester), 1988.

42 Pihlajer K & Kleinpeter E, Cabon^{-13} *chemical shifts in structure and spectrochemical analysis,* (*VCH publishers, Deerfield Beach*), 1994.

43 Karaback M, Cinar M & Kurt M, *J Mol Struct*, 982 (2010) 22.

44 Karpagam J, Sundaraganesan N, Sebastian S, Manoharan S & Kurt J, *J Raman Spectrosc*, 41 (2010) 53.

45 Vijayakumar T, Joe H, Nair C P R M & Jayakumar V S, *Chem Phys*, 343 (2008) 83.

46 Kleinman D A, *Phys Rev*, 126 (1962)1977.

47 Szafran M, Komasa A & Adamska E B, *J Mol Struct*, 827 (2007) 101.

48 James C, Raj A A, Reghunathan R, Joe I H & Jayakumar V S, *J Raman Spectrosc*, 37 (2006) 1381.

49 Jun-Na L, Zhi-Rang C, Shen-Fang Y & Zhejiang J, *Univ Sci*, 6B (2005) 584.

50 Kavitha E, Sundarabganesan N & Sebastian S, *Indian J Pure Appl Phys*, 48 (2010) 20.

51 Prasad O, Sinha L & Kumar N, *J At Mol Sci*, 1 (2010) 201.

52 http://riodbol.ibase.aist.go.jp/sbds/(National Institute of Advanced Industrial Science).